

Some Aspects of 3D Finite Element Modeling of Independent Wire Rope Core

Gordana M. Kastratović

Assistant Professor
University of Belgrade
Faculty of Transport and Traffic Engineering

Nenad D. Vidanović

Teaching Assistant
University of Belgrade
Faculty of Transport and Traffic Engineering

This paper explores some aspects of 3D modeling of independent wire rope core (IWRC). Using advanced 3D modeling techniques, finite element analysis of IWRC was investigated, with special emphasis on diverse types of contacts between wires. Several different meshed 3D models were made, and numerical analysis using finite element method based on commercial software was carried out under two different load conditions, in order to provide a better understanding, and hence prediction of the mechanical behavior of the wire ropes.

Keywords: wire rope, strand, contacts, finite element method.

1. INTRODUCTION

High strength wire ropes are very important structural members used for transmitting tensile forces. Because of their flexibility and high strength, wire ropes are in widespread use throughout the mechanical, electrical, mining and naval engineering industries. Applications include lifts, hoisting devices, electrical power transmission, aircraft arresting cables, and mining equipment.

In order to predict the wire rope behavior, several theoretical models and analytical studies have been presented in the literature, [1,2].

As technology and computer sciences were developing and became more available, numerical analyses started to be frequently used in predicting the wire rope behavior.

One of the first finite element analysis of simple straight strand has been presented by Jiang et al. in [3].

Elata et al. [4] developed a new model for simulating the mechanical response of an independent wire rope core (IWRC).

A simple straight strand based on Cartesian isoparametric formulation was presented through finite element method in [5].

A realistic 3D structural model and finite element analysis of a simple wire strand has been briefly explained in [6], by İmrak and Erdönmez. The same authors presented 3D solid model of IWRC and wire-by-wire analysis of IWCR in [7].

Most of these analyses ignored frictional effects, but there were some [3,4,7] that took those effects into consideration. However, analysis of other contact effects in IWCR was neglected in available literature. Also, all of them introduced axial loading as applied axial strain.

Because of these reasons and its complex geometry, it is still very difficult to model and analyze wire ropes, using numerical methods, such as finite element method. Also, this kind of analysis requires substantial computer resources.

Nevertheless, numerical analysis must be employed to provide a better understanding, and hence prediction, of the mechanical behavior of the wire rope strands, thus reducing the need for expensive tests (because of which the experimental results reported in the literature are very limited). In order to accomplish all of that, the aim of this paper was to explore some aspects of 3D modeling of independent wire rope core (IWRC) using the finite element method based on computer program with special emphasis on different types of contacts and different types of axial loading.

2. FINITE ELEMENT MODEL AND ANALYSIS

Model of the wire rope considered here is shown in Figure 1. As it can be seen, the cross-section of a wire rope consists of one simple, straight, seven-wire strand surrounded by six seven-wire strands. Such a cross-section is often used as a rope core in a more complex rope and as such is sometimes called an independent wire rope core or IWCR. It is a member of complex wire ropes that carries the greatest amount of axial loading.

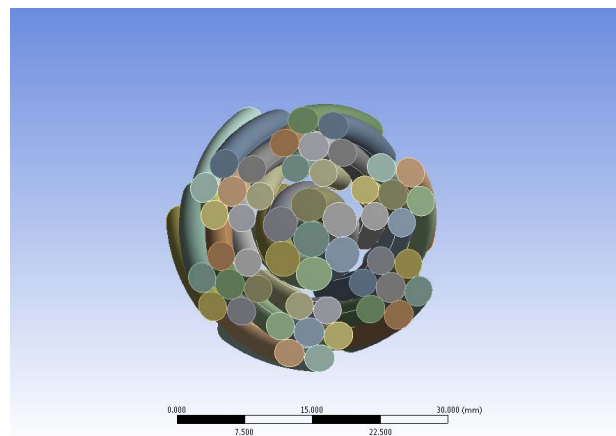


Figure 1. Cross-section of IWRC

The 3D finite element models of IWCR were created by using both CATIA and Ansys 12 Workbench. First, the parametric geometrical model was created in Generative Shape Design mode of CATIA. The obtained geometrical model was then imported as IGES format to Ansys 12 Workbench. This program allowed

Received: December 2010, Accepted: February 2011

Correspondence to: Dr Gordana Kastratović
Faculty of Transport and Traffic Engineering,
Vojvode Stepe 305, 11000 Belgrade, Serbia
E-mail: g.kastratovic@sf.bg.ac.rs

specification of material properties, generation of finite element mesh, application of loads, and contact definition as well as solving and obtaining necessary output data.

It is well known that very important issue in any finite element analysis is the element selection and mesh size. If the created mesh is too coarse, then the problem may not converge due to increased time steps and there will be no solution. On the other hand, too fine mesh may cause similar difficulty because of a large number of elements and nodes, i.e. large numbers of equations. This can also significantly increase computational time.

So, several different 3D models were made, with different numbers of elements. The goal of meshing in ANSYS Workbench is to provide robust, easy to use meshing tools that will simplify the mesh generation process. These tools have the benefit of being highly automated along with having a moderate to high degree of user control. Here, we used mesh sweeping method which is default for solid bodies. The body can be meshed very efficiently with hexahedral and wedge elements using this technique. The number of nodes and elements for a swept body is usually much smaller than ones meshed with other methods. In addition, the time to create these elements is much shorter. In this paper, a global meshing control was used to provide different number of elements, setting the basic meshing control “relevance” to three different values.

Finite element used for meshing all analyzed models was SOLID186, a brick solid element that is used in 3D modeling of solid structures, as default element. The same kind of element was used in [7], but in different software. It is a higher order 3-D 20-node solid element that exhibits quadratic displacement behavior. The element is defined by 20 nodes having three degrees of freedom per node: translations in the nodal x , y , and z directions. The element supports plasticity, hyperelasticity, creep, stress stiffening, large deflection, and large strain capabilities. It also has mixed formulation capability for simulating deformations of nearly incompressible elastoplastic materials, and fully incompressible hyperelastic materials.

SOLID186 Homogenous Structural Solid is well suited to modeling irregular meshes (such as those produced by various CAD/CAM systems), which was the case here.

Another important issue for this particular problem represents the contacts between wires and friction. Regardless of friction, contacts between wires exist and must be taken into consideration. They determine how the wires can move relative to one another and the distribution of load between them, as well, even when the friction is neglected.

The software used in this study allows two types of linear contacts, and both of them were applied in this analysis. Bonded contact is the default configuration of contact and applies to all contact regions (surfaces, solids, lines, faces, edges). If contact regions are bonded, then no sliding or separation between faces or edges is allowed, as if the bodies were *glued*. No separation contact setting is similar to the bonded case. It only applies to regions of faces (for 3-D solids) or edges (for 2-D plates). Separation of faces in contact is not allowed, but small amounts of frictionless sliding can occur along contact faces.

Also, frictional contact was available, and this nonlinear analysis was carried out, as well. In this

setting, two contacting faces can carry shear stresses up to a certain magnitude across their interface before they start sliding relative to each other. It only applies to regions of faces. This state is known as “sticking”. The model defines an equivalent shear stress at which sliding on the face begins as a fraction of the contact pressure. Once the shear stress is exceeded, the two faces will slide relative to each other. The coefficient of friction can be any non-negative value.

The axial loading behavior was analyzed, with two different load settings.

2.1 Axial loading by applying axial strain

First, axial loading behavior was investigated by applying an axial strain to the free end of the IWRC with the increments of 0.001, while the other end of the IWRC was fixed.

The IWRC 6×7 wire rope has been taken as an example. The core strand radius of center wire was $r_1 = 1.97$ mm, and outer wire $r_2 = 1.865$ mm, and pitch length 70 mm; the outer strand center wire radius was $r_3 = 1.6$ mm, and outer wire radius $r_4 = 1.5$ mm and pitch length 193 mm. The overall length of the wire rope model was 18 mm.

The model was meshed (Fig. 2), and the prescribed boundary conditions (Fig. 3) were used for solving. As mentioned, on one end of the model the degrees of freedom in all three directions were constrained, and on the other end the displacement in x and y directions were restrained to zero.

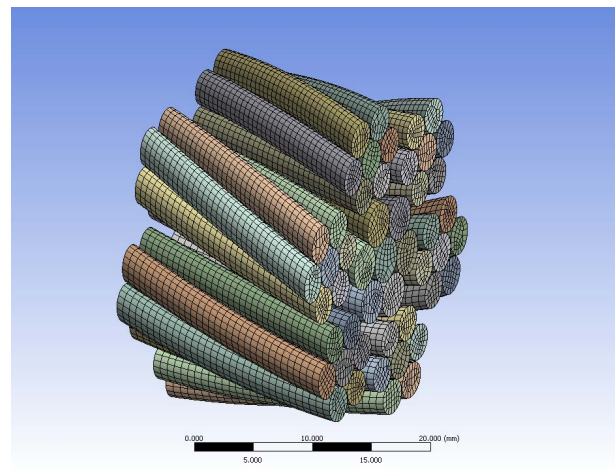


Figure 2. 3D Finite element model – mesh

It should be noted that for two types of linear contacts elastic behavior was analyzed [8]. An axial strain of 0.015 in increments of 0.001 in z direction was applied, the modulus of elasticity was $E = 1.88$ E11 Pa, and Poisson’s ratio $\nu = 0.3$.

For the model with frictional contact, nonlinear analysis was carried out. The IWRC material properties used in elastic-plastic analysis are defined as: the modulus of elasticity was $E = 1.88$ E11 Pa, Poisson’s ratio $\nu = 0.3$, yield strength $R_{p0.2} = 1.54$ E9 Pa, tangent modulus $E_t = 2.46$ E10 Pa, ultimate tensile strength $R_m = 1.8$ E9 Pa, while the friction coefficient was $\mu = 0.115$.

The described numerical models were solved, and results are presented in the following diagrams (Figs. 4, 5 and 6). To be more specific, the solutions were obtained for three different meshed models, i.e., for

298683, 616646 and 1531845 numbers of nodes or 61166, 134925 and 341925 numbers of elements respectively, for all types of contacts.

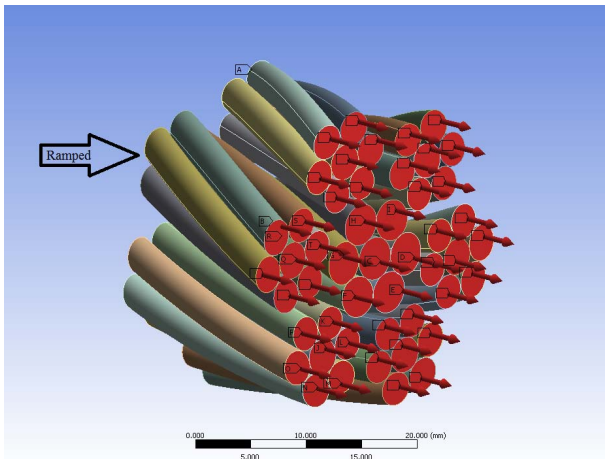


Figure 3. Boundary conditions

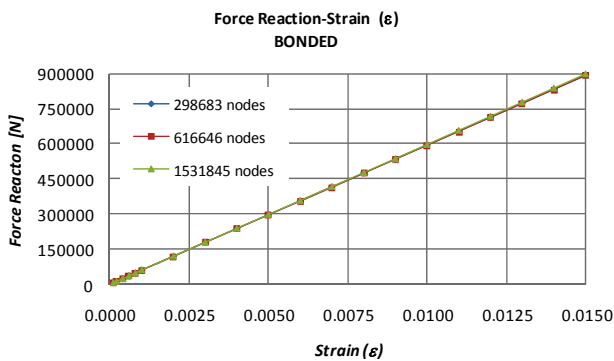


Figure 4. Diagram of resulting axial force – BONDED

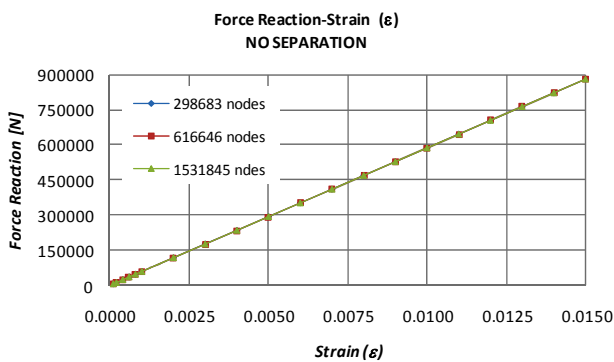


Figure 5. Diagram of resulting axial force – NO SEPARATION

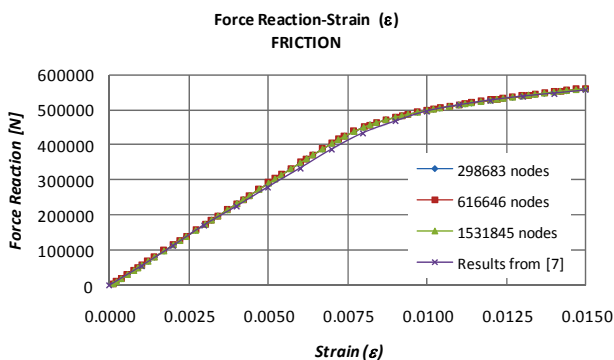


Figure 6. Diagram of resulting axial force – FRICTION

The output data in this load case were total force reaction, which was calculated as sum of all reaction forces of the individual wires.

As it can be seen in first two diagrams, there is practically no difference between results obtained for different number of nodes. Also, the diagrams show excellent agreements between obtained results and with the results from [7].

2.2 Axial loading by applying axial force

Also, axial loading behavior was investigated by applying an axial force to the free end of the same IWRC 6×7 wire rope, while the other end of the IWRC was fixed. The total force of 900 kN was applied in increments of 100 kN. The total force was evenly distributed between wires.

The other applied settings for two linear contacts, and nonlinear frictional contact were the same as in previous analysis.

Those numerical models were solved, and results are presented in the following diagrams. As before, the solutions were obtained for three different meshed models, also for 298683, 616646 and 1531845 numbers of nodes or 61166, 134925 and 341925 numbers of elements respectively, for two types of linear contact settings. For nonlinear model the solution was obtained only for 298683 number of nodes, because this type of analysis is time consuming and requires significant computer resources.

The output data in this load case were axial strain, which was calculated for each the individual wire. The applied forces are given as a function of maximal calculated strain. The maximum value of strain on the axis is 0.015 on all diagrams, which is also the case in previous load setting. This enabled comparison of the obtained results.

As it can be seen in first two diagrams (Figs. 7 and 8), there is no major difference between results obtained for different number of nodes, and that is the reason why the nonlinear model for this load case was calculated only for minimum number of nodes (Fig. 9).

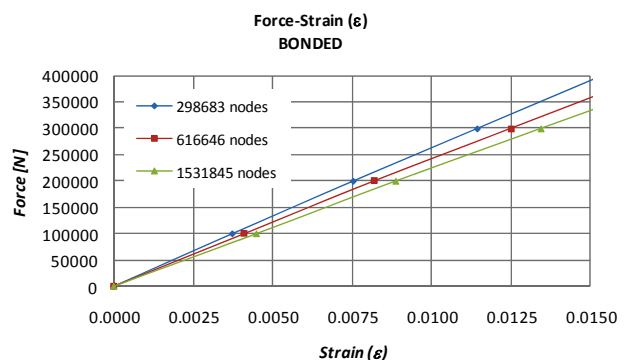


Figure 7. Diagram of applied axial force – BONDED

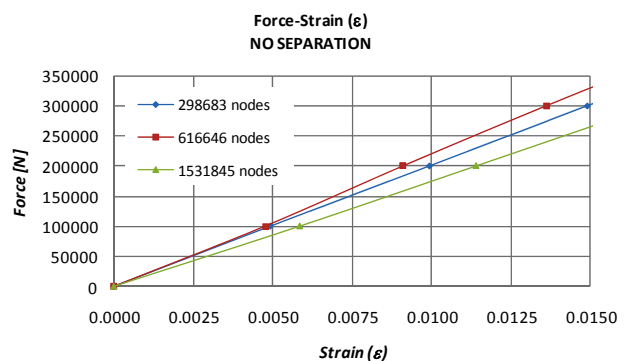


Figure 8. Diagram of applied axial force – NO SEPARATION

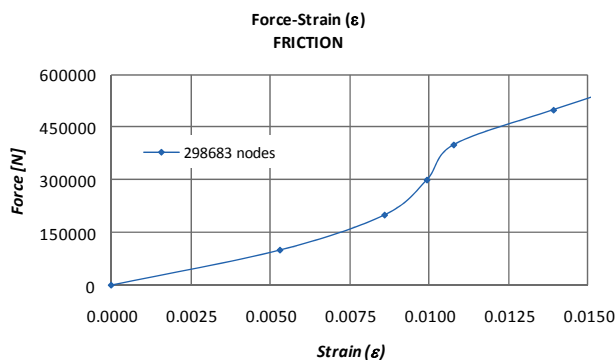


Figure 9. Diagram of applied axial force – FRICTION

It can be seen that in this case of axial loading, axial strain reaches values of 0.015 when values of applied total force reaches 300 to 400 kN. That is significantly lesser then in the previous load case.

3. COMPARISON OF THE RESULTS

The next diagram (Fig. 10) shows the comparison between results obtained in two different load cases, to be more accurate, it represents the variation of axial force with axial strain for two load cases. As it can be observed, there is discrepancy between them.

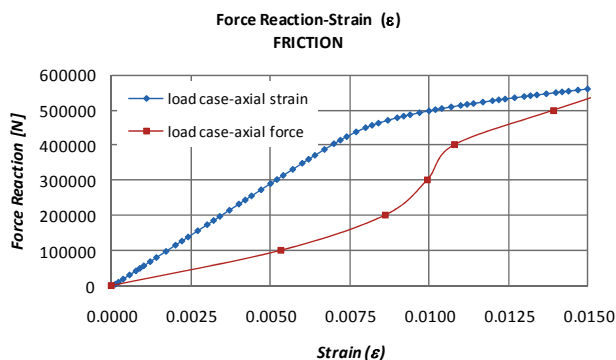


Figure 10. Variation of axial force with axial strain for two load cases

This can be assigned to the fact that the total applied force was evenly distributed between the wires, and that the obtained result for the axial strain is the maximal value of all axial strains of all the wires. This problem might be solved with more adequate force distribution between wires, and that is the topic of future analysis.

4. CONCLUSION

Using commercial software, which is currently widely available, some aspects of 3D modeling of independent wire rope core (IWRC) were investigated, using the finite element method. The wire rope was subjected to two different types of axial loading. The two different types of linear contacts between wires were applied, as well as frictional contact. It is established that there is no major difference between solutions obtained for different node numbers. The obtained results in case when the load was applied as axial strain, showed excellent agreements with the results from the literature that was available (Fig. 6). But, in the other load case, when the load was applied as axial force, there was considerable difference between results (Fig. 10). This

emphasis, ones more, the significance of creating the suitable finite element model of IWRC, in order to provide a better understanding, and hence prediction, of the mechanical behavior of the wire rope strands.

REFERENCES

- [1] Love, A.E.H.: *A Treatise on the Mathematical Theory of Elasticity*, Dover Publications, Mineola, New York, 1944.
- [2] Costello, G.A.: *Theory of Wire Rope*, Springer, Berlin, 1990.
- [3] Jiang, W.G., Henshall, J.L. and Walton, J.M.: A concise finite element model for three-layered straight wire rope strand, *International Journal of Mechanical Sciences*, Vol. 42, No. 1, pp. 63-86, 2000.
- [4] Elata, D., Eshkenazy, R. and Weiss, M.P.: The mechanical behavior of a wire rope with an independent wire rope core, *International Journal of Solids and Structures*, Vol. 41, No. 5-6, pp. 1157-1172, 2004.
- [5] Sun, J.-F., Wang, G.-L. and Zhang, H.-O.: Elastoplastic contact problem of laying wire rope using FE analysis, *The International Journal of Advanced Manufacturing Technology*, Vol. 26, No. 1-2, pp. 17-22, 2005.
- [6] Erdönmez, C. and İmrak, C.E.: Modeling and numerical analysis of the wire strand, *Journal of Naval Science and Engineering*, Vol. 5, No. 1, pp. 30-38, 2009.
- [7] İmrak, C.E. and Erdönmez, C.: On the problem of wire rope model generation with axial loading, *Mathematical and Computational Applications*, Vol. 15, No. 2, pp. 259-268, 2010.
- [8] Kastratović, G. and Vidanović, N.: The analysis of frictionless contact effects in wire rope strand using the finite element method, *Transport & Logistics*, No. 19, pp. 33-40, 2010.

ПОЈЕДИНИ АСПЕКТИ 3Д МОДЕЛОВАЊА ЧЕЛИЧНИХ УЖАДИ СА НЕЗАВИСНИМ ЧЕЛИЧНИМ ЈЕЗГРОМ МЕТОДОМ КОНАЧНИХ ЕЛЕМЕНАТА

Гордана М. Кастратовић, Ненад Д. Видановић

У овом раду су разматрани поједини аспекти 3Д моделовања челичних ужади са независним челичним језгром (IWRC). Користећи се напредним техникама 3Д моделирања, а методом коначних елемената, анализирано је независно челично језгро, са посебним освртом на различите типове контаката између влакана. Креирано је неколико 3Д модела са различитим мрежама коначних елемената и спроведена је нумеричка анализа комерцијалним софтвером за два различита типа оптерећења, а у циљу бољег разумевања, а тиме и предвиђања, механичког понашања челичних ужади.